

An evaporation estimation method based on the coupled 2-D turbulent heat and vapor transport equations

Jozsef Szilagyi^{1,2} and Janos Jozsa¹

Received 14 July 2008; revised 4 December 2008; accepted 7 January 2009; published 17 March 2009.

[1] The analytical solution of the coupled turbulent diffusion equations of heat and vapor transport across a moisture discontinuity under near-neutral atmospheric conditions and constant energy available at the evaporating surface yields a simple equation (i.e., the wet-surface equation [WSE]) that relates the change in surface temperature to the change in the land surface moisture content as the environment dries. With the help of percent possible sunshine, air temperature, and humidity measurements at selected weather stations as well as land surface temperature values from MODIS data, monthly, warm-season evaporation rates were estimated for five rectangular regions across the contiguous U.S. employing the WSE. The so-derived monthly evaporation rates correlated very strongly ($R^2 = 0.95$) with traditional complementary relationship-derived evaporation estimates using the same weather-station data. Even on an annual basis the correlation remained unchanged. WSE with no tunable parameters may in the future help in calibration and validation of other evaporation estimation techniques that may or may not rely on land surface temperature data.

Citation: Szilagyi, J., and J. Jozsa (2009), An evaporation estimation method based on the coupled 2-D turbulent heat and vapor transport equations, *J. Geophys. Res.*, 114, D06101, doi:10.1029/2008JD010772.

1. Introduction

[2] Over the past several decades there has been a rapid expansion in the number of evaporation estimation algorithms using remotely sensed characteristics of the evaporating surface, such as its temperature or its vegetation cover and status. For a review of the current approaches see the works of *Gowda et al.* [2008] and *Courault et al.* [2005]. A common characteristic of these remote-sensing-based methods is that they all contain varying number of parameters that must be calibrated. Any parameter calibration contains inherent uncertainties of whether the calibrated value is really of an optimum in a predefined sense. With the number of parameters this uncertainty increases fast because of typically unknown interactions between the parameters, potentially leading to so-called parameter equifinality, as became known in hydrology, meaning that often widely differing combinations of the parameter values result in almost identical model output, thus defining an optimal set of the parameters ambiguous.

[3] Since estimated “large-scale” areal evaporation rates of the above models can only be validated with measurements (such as obtained at flux towers or lysimeters) typically representative over a much smaller scale (i.e., field scale), an areal evaporation technique that works at the same

“large scale” and does not have any tunable parameters may be a useful tool in calibration and verification of the former approaches. Even for those models that nowadays give results at a resolution that corresponds to the field scale [e.g., *Allen et al.*, 2007; *Anderson et al.*, 2007; *Agam et al.*, 2008], an independent “large-scale” comparison/validation may be advantageous.

[4] The areal evaporation estimation technique discussed below is based on the coupled 2-D turbulent heat and vapor transport equations with known analytical solutions by *Laikhtman* [1964] and *Yeh and Brutsaert* [1971]. These fairly general solutions will be considered under the constraint that the energy at the land surface available for heat conduction into the soil, as well as for latent and sensible heat transfer across the land-atmosphere interface, remains quasi-constant as the originally wet land around a permanently wet patch dries out. The result is a simple equation with well-defined physical parameters that connects the change in land surface moisture content to the ensuing change in surface temperature over the drying land. The analytical solutions assume a uniform roughness of the land surface across the moisture discontinuity, which may not be valid in practical applications when the moist surface is represented by open water, such as a shallow lake. The application of e.g., large-eddy simulation (LES) models [*Leclerc et al.*, 1997; *Albertson and Parlange*, 1999; *Albertson et al.*, 2001; *Kustas and Albertson*, 2003] could reveal the effect of a sudden jump in land surface properties (other than the temperature and moisture status) on the accuracy of the above analytical solutions under these more relaxed conditions. Such a comparison, to the best of the

¹Department of Hydraulic and Water Resources Engineering, Budapest University of Technology and Economics, Budapest, Hungary.

²School of Natural Resources, Lincoln Conservation and Survey Division, University of Nebraska, Lincoln, Nebraska, USA.

authors' knowledge, has not been completed and is not included in the present study.

2. Coupled, 2-D Turbulent Heat and Vapor Transport Equations, Their General and Constraint Analytical Solutions

[5] Let's consider a sudden moisture and temperature discontinuity of the land surface along the x axis of a Cartesian coordinate system. Let's assume that perpendicular to the prevailing mean wind, \bar{u} , blowing along the x axis, nothing changes, i.e., for any variable, Φ , and value of y , $\Phi(x, y) = \Phi(x, 0)$. Since everything is assumed to be constant along the y axis, the other two components of the mean wind vector can be considered zero without loss of generality. Let us denote by K_v and K_h the vertical tensor components of the turbulent diffusivity for vapor and heat, and assume that they are similar in value, i.e., $K_v \approx K_h = K$. By applying a first-order closure approach for the turbulent fluxes the steady vapor and heat transport equations become

$$\begin{aligned} \bar{u} \frac{\partial \bar{q}}{\partial x} &= \frac{\partial}{\partial z} \left(K \frac{\partial \bar{q}}{\partial z} \right) \\ \bar{u} \frac{\partial \bar{T}}{\partial x} &= \frac{\partial}{\partial z} \left(K \frac{\partial \bar{T}}{\partial z} \right) \end{aligned} \quad (1)$$

where \bar{q} is the mean specific humidity, \bar{T} is the mean air temperature, a good approximation for the required mean potential temperature because of the close proximity to the land surface. The surface roughness is further assumed to be uniform, while the prescribed equilibrium $\bar{u}(z) = az^m$ and $K(z) = bz^n$ profiles are supposed to remain unchanged in time and space across the discontinuity. From experimental data $a = (5.5/7m) u_* (z_0)^{-m}$, $b = u_* z_0^m / (5.5m)$ and $n = 1 - m$ can be written [e.g., *Brutsaert*, 1982], where u_* is the friction velocity and z_0 the roughness height of the surface, but they are not needed to be specified this way for the solution of equation (1).

[6] Upwind of the discontinuity (from here on the sub-script "a" will refer to the nonwet "arid" conditions) let the specific humidity, $\bar{q}_a(z)$, and temperature, $\bar{T}_a(z)$, profiles be in an equilibrium

$$\frac{\partial}{\partial z} \left(K \frac{\partial \bar{T}_a}{\partial z} \right) = \frac{\partial}{\partial z} \left(K \frac{\partial \bar{q}_a}{\partial z} \right) = 0. \quad (2)$$

At the fully saturated wet surface, i.e., $0 < x < x_f$, the specific humidity is, of course, a function of its temperature, although this is not a necessary assumption for the solution. Here x_f is the extent (or fetch) of the wet patch along the x axis. Let also the net energy flux be zero at the surface everywhere, while let the incident radiation, R_{da} and R_d , at the surface be constant, however, not necessarily the same over the drying land and the permanently wet patch, because of possible differences in the albedo as a result of the moisture contrast. The thermal radiation of the surface, treated as a grey body with emissivity, ε , is a function of its temperature, given by the Stefan-Boltzmann law. Let's assume here that heat conduction at the surface, G_a and G (for $x_f < x$ and $x \leq 0$ as well as $0 < x \leq x_f$, respectively) into the soil is constant [*Laikhtman*, 1964], although they may depend on the surface temperature, as discussed by *Yeh and Brutsaert* [1971] who formulated the solution of

equation (1) for this latter, more general case too (not considered here).

[7] Let now the boundary conditions (BC) be defined first for the "arid" surface

$$\begin{aligned} \bar{q}_a &= q_{as}, \quad \bar{T}_a = T_{as} && \text{at } z = 0 \\ -c_p \rho K \frac{\partial \bar{T}_a}{\partial z} - L_e \rho K \frac{\partial \bar{q}_a}{\partial z} + \varepsilon \sigma T_{as}^4 + G_a &= R_{da} && \text{at } z = 0 \\ -c_p \rho K \frac{\partial \bar{T}_a}{\partial z} &= H_a, \quad -\rho K \frac{\partial \bar{q}_a}{\partial z} &= E_a, && \text{at } z = 0 \end{aligned}$$

and then for the wet surface

$$\begin{aligned} \bar{q} &= \bar{q}_a(z), \quad \bar{T} = \bar{T}_a(z) && \text{at } x = 0, z > 0 \\ q &= q_s(T_s) && \text{at } 0 < x < x_f, z = 0 \\ -c_p \rho K \frac{\partial \bar{T}}{\partial z} - L_e \rho K \frac{\partial \bar{q}}{\partial z} + \varepsilon \sigma T_s^4 + G &= R_d && \text{at } 0 < x < x_f, z = 0 \\ -c_p \rho K \frac{\partial \bar{T}}{\partial z} &= H_a, \quad -\rho K \frac{\partial \bar{q}}{\partial z} &= E_a && \text{at } x > x_f, z = 0 \end{aligned}$$

where c_p is the specific heat of air at constant pressure, L_e the latent heat of vaporization of water, σ the Stefan-Boltzmann constant, ρ the air density, H_a and E_a the heat and water vapor fluxes from the land surface up- and downwind of the wet patch. Note that only either T_{as} or q_{as} can be arbitrary, since for a given R_{da} and G_a they together must satisfy the second BC of the arid surface.

[8] Equation (1) with the specified equilibrium profiles and BCs was first solved analytically by *Laikhtman* [1964] and later, including the more general soil heat conduction case, by *Yeh and Brutsaert* [1971]. Let the following terms be defined as

$$\begin{aligned} c_1 &= c_p \rho b (T_m - T_{as}) \left(\frac{a}{bx_f} \right)^\nu (1-n)^{1-2\nu} \\ c_2 &= 4\varepsilon \sigma T_{as}^3 (T_m - T_{as}) \\ c_3 &= L_e \rho b (q_m - q_{as}) \left(\frac{a}{bx_f} \right)^\nu (1-n)^{1-2\nu} \\ c_4 &= (R_d - G) - (R_{da} - G_a) \\ c_5 &= \frac{T_m - T_{as} dq^*}{q_m - q_{as} dT} \Big|_{T=\langle T \rangle} = \frac{T_m - T_{as}}{q_m - q_{as}} \alpha_q \\ c_6 &= \frac{q_{as}^* - q_{as}}{q_m - q_{as}} \\ \omega &= \frac{c_2 \nu^{1-2\nu} \Gamma(\nu)}{(c_1 + c_3 c_5) \Gamma(1-\nu)} \end{aligned}$$

where T_m and q_m are some representative temperature and specific humidity of the wet surface, $\nu = (1-n)/(2+m-n)$, Γ is the complete gamma function, and q^* is a point on the saturated specific humidity curve, the slope of which, α_q , is to be evaluated at the below specified temperature, $\langle T \rangle$. With the above terms the water vapor and heat flux from the wet surface can be obtained as [*Yeh and Brutsaert*, 1971]

$$\begin{aligned} E &= -\rho K \frac{\partial \bar{q}}{\partial z} \Big|_{z=0} = E_a + c_p \rho b \left(\frac{a}{bx_f} \right)^\nu (1-n)^{1-2\nu} \\ &\cdot \frac{q_{as}^* - q_{as}}{\Gamma(\nu) \nu^{1-2\nu} (c_p + \alpha_q L_e)} \xi^{-\nu} + \frac{\alpha_q [c_4 + c_2 c_3 c_6 / (c_1 + c_3 c_5)]}{c_p + \alpha_q L_e} \\ &\cdot \sum_{i=0}^{\infty} \frac{(-\omega)^i \xi^{i\nu}}{\Gamma(1+i\nu)} \end{aligned} \quad (3)$$

$$\begin{aligned}
H = & -c_p \rho K \frac{\partial \bar{T}}{\partial z} \Big|_{z=0} = H_a - c_p \rho b \left(\frac{a}{bx_f} \right)^\nu (1-n)^{1-2\nu} \\
& \cdot \frac{L_e(q_{as}^* - q_{as})}{\Gamma(\nu)\nu^{1-2\nu}(c_p + \alpha_q L_e)} \xi^{-\nu} + \frac{c_p[c_4 + c_2 c_3 c_6 / (c_1 + c_3 c_5)]}{c_p + \alpha_q L_e} \\
& \cdot \sum_{i=0}^{\infty} \frac{(-\omega)^i \xi^{i\nu}}{\Gamma(1+i\nu)} \quad (4)
\end{aligned}$$

where $\xi = x/x_f$. The temperature and specific humidity of the wet surface results as [Yeh and Brutsaert, 1971]

$$\begin{aligned}
T_s = & T_{as} - \frac{L_e(q_{as}^* - q_{as})}{c_p + \alpha_q L_e} \\
& + \frac{\nu^{1-2\nu} \Gamma(\nu)[c_4 + c_2 c_3 c_6 / (c_1 + c_3 c_5)]}{\Gamma(1-\nu)\rho b [a/(bx_f)]^\nu (1-n)^{1-2\nu} (c_p + \alpha_q L_e)} \\
& \times \sum_{i=0}^{\infty} \frac{(-\omega)^i \xi^{\nu+i\nu}}{\Gamma(1+\nu+i\nu)} \quad (5)
\end{aligned}$$

$$\begin{aligned}
q_s = & q_{as} + \frac{c_p(q_{as}^* - q_{as})}{c_p + \alpha_q L_e} \\
& + \frac{\alpha_q \nu^{1-2\nu} \Gamma(\nu)[c_4 + c_2 c_3 c_6 / (c_1 + c_3 c_5)]}{\Gamma(1-\nu)\rho b [a/(bx_f)]^\nu (1-n)^{1-2\nu} (c_p + \alpha_q L_e)} \\
& \times \sum_{i=0}^{\infty} \frac{(-\omega)^i \xi^{\nu+i\nu}}{\Gamma(1+\nu+i\nu)}. \quad (6)
\end{aligned}$$

For the full solution describing $\bar{T}(x, z)$ and $\bar{q}(x, z)$ over the wet surface, see the work of Laikhtman [1964] or Yeh and Brutsaert [1971].

[9] By assuming that at the surface (including both the drying and wet surface) the available energy, Q_n , rather than R_d or R_{da} , stays quasi-constant in space and time as the originally uniformly wet area dries out for $x \leq 0$ (and also for $x > x_f$), i.e., $Q_n = R_{da} - G_a - \varepsilon \sigma T_{as}^4 = R_d - G - \varepsilon \sigma T_s^4 \approx \text{const.}$, the thermal radiation and soil heat conduction terms drop out of the BCs (since this way they never get defined), and so do the c_2 and c_4 terms as well, the latter because both R_{da} and R_d now become replaced by the same constant Q_n . As a consequence, the third terms of the right hand side (r.h.s.) of equations (3)–(6) vanish too, yielding

$$\begin{aligned}
E = & -\rho K \frac{\partial \bar{q}}{\partial z} \Big|_{z=0} \\
= & E_a + c_p \rho b \left(\frac{a}{bx_f} \right)^\nu (1-n)^{1-2\nu} \cdot \frac{q_{as}^* - q_{as}}{\Gamma(\nu)\nu^{1-2\nu}(c_p + \alpha_q L_e)} \xi^{-\nu} \quad (7)
\end{aligned}$$

$$\begin{aligned}
H = & -c_p \rho K \frac{\partial \bar{T}}{\partial z} \Big|_{z=0} \\
= & H_a - c_p \rho b \left(\frac{a}{bx_f} \right)^\nu (1-n)^{1-2\nu} \cdot \frac{L_e(q_{as}^* - q_{as})}{\Gamma(\nu)\nu^{1-2\nu}(c_p + \alpha_q L_e)} \xi^{-\nu} \quad (8)
\end{aligned}$$

$$T_s = T_{as} - \frac{L_e(q_{as}^* - q_{as})}{c_p + \alpha_q L_e} \quad (9)$$

$$q_s = q_{as} + \frac{c_p(q_{as}^* - q_{as})}{c_p + \alpha_q L_e}. \quad (10)$$

[10] Note that equation (7) when averaged over the fetch is the solution of Sutton's problem as described by Brutsaert [1982]. From equations (7) and (8), this way, the sensible, H , and latent heat fluxes, LE , change at the same rate along the wet surface, but opposite in sign, since equation (7) multiplied by L_e yields the same second term on the r.h.s. as equation (8). From equation (9) it furthermore follows that the temperature of the wet surface is constant along the fetch and must remain constant through time as well (under a temporally constant Q_n and unchanged $\bar{u}(z)$ and $K(z)$ profiles), since the transported heat from the drying land toward the wet patch is fully consumed by an increased evaporation rate from it as equations (7) and (8) predict. In other words, a constant wet-surface temperature along the wet patch from equation (9) means that any point of the wet surface, even if it is located infinitely far along the patch, should respond (in terms of its temperature) the same way to an increased upwind aridity of the environment. This certainly cannot happen as the air temperature and humidity of an air parcel will change along the fetch as it is being blown over the wet surface, thus sooner or later blending into the air above the wet patch, which thus remains unaffected by the aridity change upwind, infinitely far away. Therefore a spatially constant temperature along the wet patch, as equation (9) predicts under a constant Q_n term, can only be maintained during drying of the surrounding environment if it remains the same constant in time as well. This conclusion has already been drawn speculatively by Morton [1983] and more recently by Szilagyi and Jozsa [2008]. While Yeh and Brutsaert [1971] and Brutsaert [1982] also discussed this possibility of a balance in the sensible and latent heat fluxes along the wet surface and therefore a spatially constant wet-surface temperature, they did not explicitly specify when could this be physically expected, i.e., when Q_n is constant in space, neither did they conclude that the wet-surface temperature must remain constant in time under a temporally constant Q_n (and unchanged $\bar{u}(z)$ and $K(z)$ profiles) assumption.

[11] Dividing equation (9) by equation (10), the following equation results

$$\frac{T_s - T_{as}}{q_s - q_{as}} = -\frac{L_e}{c_p} = \frac{\Delta T_{as}}{\Delta q_{as}} \quad (11)$$

which is similar to the wet-bulb equation (hence let it be called wet-surface equation [WSE]) written now for the land surface. The equation on the l.h.s. of equation (11) has been published by Yeh and Brutsaert [1971], but not the r.h.s. with its temporal changes (Δ) that follow from a temporally constant wet-surface temperature realization under a constant Q_n , provided the region was uniformly wet initially. Equation (11) this way relates the change in land surface temperature to an accompanying change in its surface moisture status and, thus, can help with actual evaporation estimation when the land surface temperature is monitored. With additional Q_n , or in lieu of it, percent possible sunshine (PPS), air temperature and humidity measurements sensible and latent heat fluxes can therefore be derived.

[12] In equation (11), for any constant T_s in time, either T_{as} or q_{as} can be specified and the other calculated. However, when the so-derived pair of T_{as} and q_{as} values is substituted back into equations (9) and (10) with α_q

Table 1. Surface Temperature, T_{as} , Values to Prescribed Values of q_{as} in Equation (11) as Well as the Back-Calculated Values in Equation (9) With α_q Evaluated at T_{as} and $(T_{as} + T_m)/2$ ^a

$q_{as} = cq^*(T_m), c$	T_{as} (°C) From Equation (11)	T_s (°C) From Equation (9) With $\alpha_q(T_{as})$	T_s (°C) From Equation (9) With $\alpha_q[(T_{as} + T_m)/2]$
0.95	21.75	20.06	20
0.9	23.5	20.22	19.99
0.85	25.26	20.5	19.99
0.8	27	20.86	19.98

^a $T_m = 20$ °C, the star denotes the saturation value of q .

evaluated at T_{as} as defined by *Yeh and Brutsaert* [1971], a large difference in the T_s values between equations (9) and (11) can be observed (Table 1) whenever the $T_{as} - T_s$ or $q_{as} - q_s$ difference itself is large. This is so because the derivation of the analytical solution of equation (1) is based on a linearization that requires the temperature (and humidity) change at the drying surface to be small. The discrepancy can however be minimized if α_q is evaluated at $\langle T \rangle = (T_{as} + T_m)/2$. This temperature replacement is expected to only slightly affect the numerical values of the analytical solution.

3. Application of the Wet-Surface Equation for Evaporation Estimation

[13] To demonstrate the applicability of equation (11) for practical regional evaporation estimation purposes in different climate and land cover environments, widely available remotely sensed land surface temperature (LST) data products were sought out. The freely available MODIS data of atmospherically corrected daytime LST, with a spatial resolution of about 1 km and a temporal coverage of at least seven years, seemed to be an ideal choice. The eight-day composited LST images employed in this study further minimize the blocking effects of clouds and make an almost continuous LST record possible around the sites selected in this study.

[14] Site selection was based on climatic data availability. All 300 stations, listed in the National Climatic Data Center's US-Local Climatological Data Publication online archive, were individually perused for monthly percent possible sunshine, air temperature, and humidity records. As it turned out, the PPS values, needed for estimating the

available energy at the surface, became the limiting factor. Out of the 300 stations, altogether nine (Austin, Texas; Burlington, Vermont; Des Moines, Iowa; Dodge City, KS; North Little Rock, AR; North Platte, Nebraska; Sioux Falls, South Dakota; Syracuse, New York; Wichita, Kansas) were found that had monthly PPS values over the 2000–2006 (2000–2005 for North Little Rock) period, the available temporal coverage of the MODIS data. The station at Burlington, Vermont, lies next to Lake Champlain, which creates an undesired discontinuity in the required environmental conditions, since the derivation of WSE (i.e., [12]) assumes a homogeneous land area.

[15] The weather station at North Platte, Nebraska is close to the Sand Hills, a unique grass-covered sand dune region in the western hemisphere. Due to the sandy and very permeable soils, no extensive irrigation takes place within the Sand Hills (but not so in its flanks), which thus ensures a fairly homogeneous area in terms of soil type, vegetation cover, and, thus, soil moisture, even though over the dunes the grass cover maybe sparser and in the interdunal valleys thicker because of the convergence (and shallower depth) of groundwater there that is being replenished over the dunes. Moreover, the area is dotted with numerous shallow lakes that can serve as a proxy for obtaining the wet-surface temperature required by equation (11). Note that wet areas could be identified by irrigated crops, however, the roughly 1-km resolution of the MODIS data precludes the employment of central-pivot irrigation circles so prevalent in Nebraska. The Crescent Lake Wildlife Refuge just west of North Platte (Figure 1) contains several shallow lakes that are large enough in size that they show up in the MODIS pixels. While open water has a different albedo and emissivity than vegetated land, and thus a different Q_n term, it is

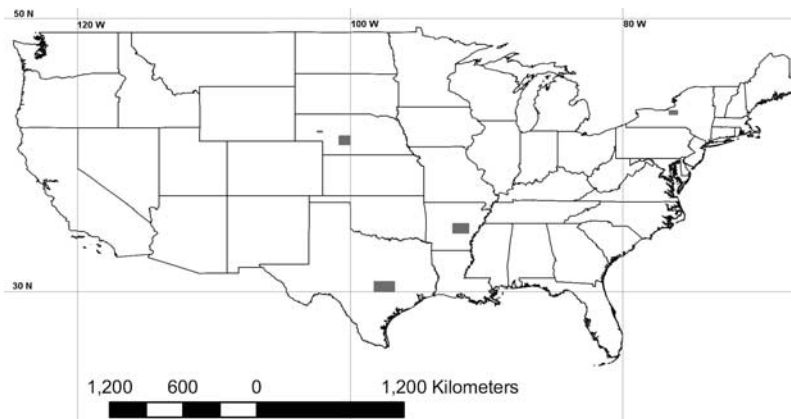


Figure 1. Location and extent of the five rectangular areas evaporation is estimated for. From left to right: Crescent Lake (Nebraska); North Platte (Nebraska); Austin (Texas); Little Rock (Arkansas); Syracuse (New York).

Table 2. Ancillary Data Used in the Study, as Well as Warm-Season Averaged Mean Monthly Evaporation Rates (E) by the WSE- and CR-Based AA Methods

Weather Station (WBAN #)	Period of Record	Area Coordinates (degrees) Upper Left Corner, Lower Right Corner	MODIS Grid Size (Row, Column)	Grid Coordinates of Wet Cell (Row, Column), and Name of Lake	E (mm/month)
Scottsbluff, NE (24028)	June–November, 2000–2006	Crescent Lake (-102.4, 41.75) (-102.05, 41.63)	(9, 20)	(4, 1–2) Crescent Lake	$E_{WSE} = 91$ $E_{CR} = 87$
North Platte, NE (24023)		North Platte (-100.83, 41.4) (-100, 0.40.75)	(46, 50)	(26–27, 4) Lake Maloney	$E_{WSE} = 96$ $E_{CR} = 103$
Syracuse, NY (14771)	June–October, 2000–2006	(-76.6, 43.25) (-76.0, 42.94)	(27, 53)	(29, 97) Oneida Lake Circular mask center: (16,43) Radius (in cells): 7	$E_{WSE} = 97$ $E_{CR} = 90$
North Little Rock, AR (03952); Little Rock, AR (13963)	June–November, 2000–2005	(-92.5, 35.0) (-91.3, 34.3)	(69, 118)	(8, 54) and (8, 56) Peckerwood Lake	$E_{WSE} = 148$ $E_{CR} = 147$
Austin, TX (13904)	June–November, 2000–2006	(-98.25, 30.75) (-96.75, 30.0)	(77, 154)	Lake Georgetown	$E_{WSE} = 127$ $E_{CR} = 131$

provisionally assumed here that this difference is not detrimental for the ensuing analysis. The situation maybe alleviated for shallow lakes that has significant phragmite cover, such as the ones at Crescent Lake. Shallowness of the lake is important in its energy balance, as with depth a lake responds increasingly sluggish to changes (e.g., seasonal) in external energy inputs.

[16] From the eight-day composited daytime LST values a monthly mean value was calculated at each pixel. A mean daytime wet LST of each month was obtained by simple averaging of the pixels (Table 2) that overlay the designated lake. A mean daytime drying LST was similarly obtained each month from the nonwet pixels (Figure 2). Saturated specific humidity in equation (11) was calculated as

$$q_s = \frac{0.622}{p} 6.11 \exp[17.27T_s/(237.3 + T_s)] \quad (12)$$

where T_s is the mean monthly daytime wet LST in Celsius. The resulting q_{as} values from equation (11) were converted into vapor pressure, e_{as} , by multiplying them with the measured mean monthly atmospheric pressure, p , and dividing by 0.622. The monthly evaporation rate, E_{WSE} , was finally obtained as $E_{WSE} = Q_n/(Bo + 1)$ where Bo is the Bowen ratio, calculated as $Bo = \gamma(T_{as} - T_{dt})/(e_{as} - e_{dt})$, γ being the psychrometric constant, defined as $\gamma = pc_p/(0.622L_e)$, T_{dt} and e_{dt} are the daytime air temperature and vapor pressure values and Q_n (specified in mm/month) was obtained by WREVAP [Morton *et al.*, 1985]. Note that the WREVAP program calculates net radiation at the land surface, which for a time period equal or longer than a day can typically be regarded as Q_n . The same large time period further ensures that the near-neutral atmospheric stability requirement for the applicability of equation (11) is also met.

[17] Since the MODIS LST values were derived for the day, a transformation of the daily mean air temperature (T_d) values (averaged for the month) has been necessary for obtaining the mean daytime temperatures (T_{dt}) as $T_{dt} = T_d + k(T_{max} - T_d)$, where T_{max} is the reported daily maximum temperature (again averaged for the month), and k is an adjustment factor, a function of latitude (Φ) and season. First the length of the daytime (in radian) is calculated as twice of the sunset angle, ω (radian, relative to noon). The latter is defined as $\omega = \arccos[-\tan(\Phi)\tan(\delta)]$ with $\delta = 0.4093 \sin(2\pi J/365 - 1.405)$ where J is the Julian date of the middle day of the month [e.g., Maidment, 1993]. Then it was assumed that the daily temperature signal (T) is sinusoid with an amplitude of $A(= T_{max} - T_d)$ and peak around 3 pm, i.e., $T = A\sin(t - 3\pi/4)$ with the time of the day, t , given in radian. The value of k then was obtained as the mean of this signal (i.e., its integral divided by the integration interval) over the daytime period of $(\pi - \omega, \pi + \omega)$ divided by A . Furthermore, the e_{dt} values in the Bowen ratio were obtained from the mean of the reported (typically at 6 am, noon, and 6 pm) daytime relative humidity, RH_{dt} , values multiplied by the saturated vapor pressure at T_{dt} .

[18] The resulting monthly evaporation rates were compared to similar estimates (Figure 3) of the Advection Aridity (AA) model [Brutsaert and Stricker, 1979]. AA

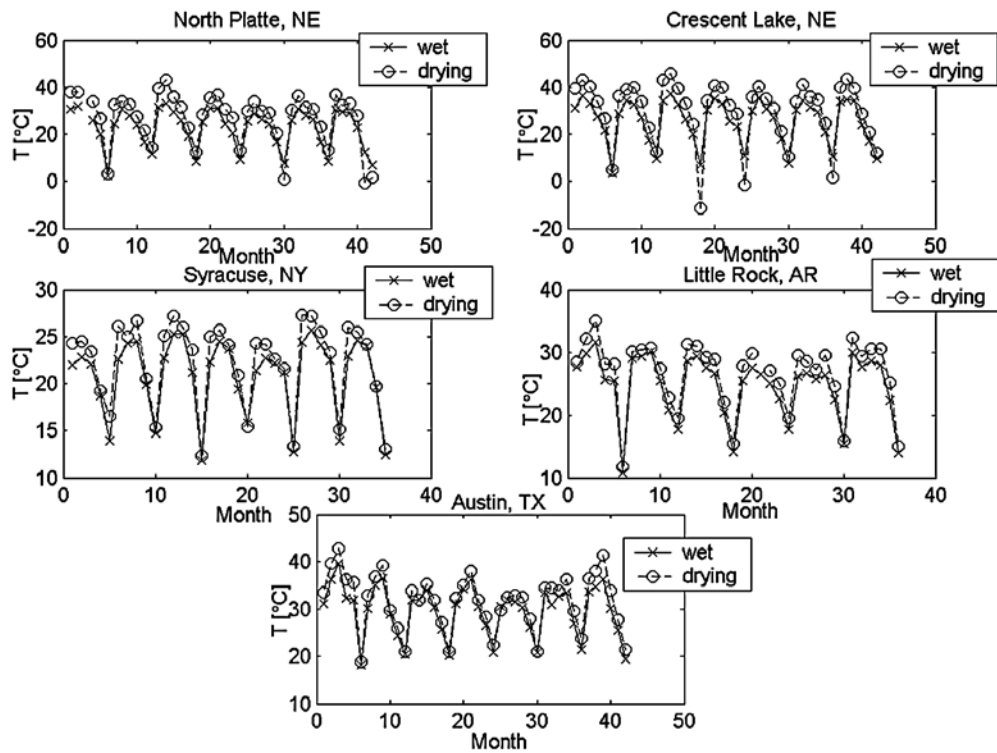


Figure 2. Mean monthly warm-period daytime surface temperatures of the (a) five rectangular drying areas and (b) permanently wet MODIS cells located within the rectangles. See Table 2 for further details.

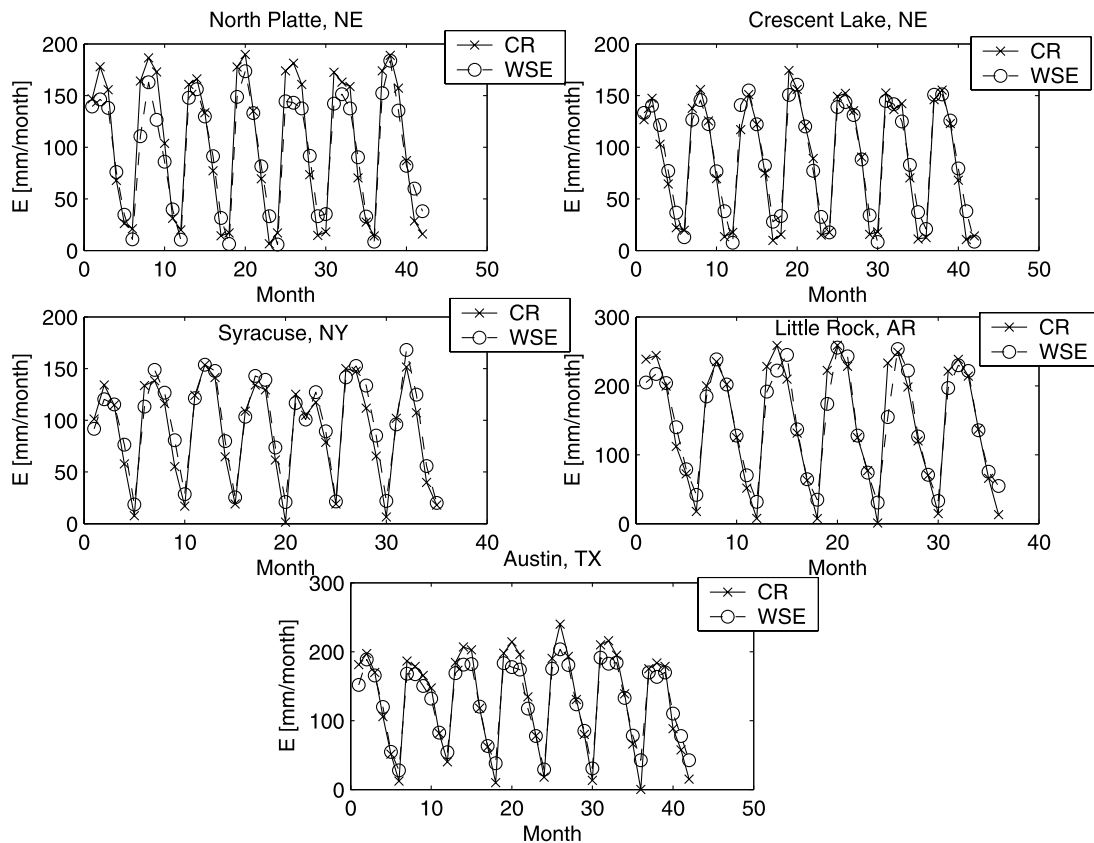


Figure 3. Monthly warm-period evaporation estimates based on (a) the wet-surface equation (WSE) and (b) the CR-based AA model (CR).

utilizes the complementary relationship, CR, [Bouchet, 1963] of evaporation and requires the same net radiation, air temperature and humidity data (but not the LST) that were used for calculating E_{WSE} besides wind velocity measurements which were also available at the selected stations or at nearby ones. The AA model has only one free parameter, the Priestley-Taylor coefficient [Priestley and Taylor, 1972], the value of which was set to be 1.29 throughout this study. Typically this parameter has a value between 1.2 and 1.3. As previously has been found by Szilagyi and Jozsa [2008] and has also been confirmed here, the AA model tends to yield negative evaporation values in cold months, thus in such months the AA-model estimates have been replaced by similar estimates of the WREVAP model, which does not exhibit this problem. However, WREVAP does not rely on the available wind measurements which prompted the overall adoption of the AA model in this study to verify the WSE-based evaporation estimates.

[19] Encouraged by the results for the Crescent Lake area (Figure 3 and Table 2), the calculations were repeated for four other areas (Figure 1) surrounding the weather stations: North Platte (Nebraska), Austin (Texas), North Little Rock (with wind measurements from Little Rock, Arkansas), and Syracuse (New York), which are less homogeneous in their land properties. In the selection of these four additional sites from the possible eight listed above, it was attempted to cover climatic and vegetation conditions as wide as possible. Dodge City, Wichita, North Platte, Sioux Falls, and Des Moines are all situated in the broader midwest area with similar climatic and vegetation conditions, so only one site was chosen (i.e., North Platte, Nebraska) from this group.

[20] From the five sites (Figure 1) selected, it turned out that the area around Syracuse is the most heterogeneous, the city standing out with very high surface temperatures in the summer from the rest of the area. Consequently, based simply on visual inspection of the MODIS images, a circle with a radius of 7 pixels in size, centered over the city (Table 2), was used to block out pixels in the drying LST calculations.

[21] In the wet pixel selections, it was attempted to choose the smallest identifiable (i.e., on the MODIS image) shallow water body, and if possible, of a natural lake with minimal in- and outflow, rather than typically deeper reservoirs with large in- and outflows. In the lack of that, only those few pixels were selected that lie near the shore of a larger and deeper water body, such as Oneida Lake in New York. Selection of more than one wet pixel may be necessitated by the residual cloud effects in the MODIS values occasionally giving erroneous (typically a warm-season value of smaller than -20°C) LST values. Such values were filtered out before the E_{WSE} calculations.

[22] Finally, in the rectangular area selection around a given weather station, the mean wind direction was accounted for, to make sure that the station would have a fetch from the area the LST is predominantly calculated for. The actual size of the area was influenced by capturing at least a few pixels of a shallow water body within clearly discernible in the MODIS image, but at the same time exclude, as much as possible, any surplus or additional water bodies. That is why, for example, around Syracuse, only the western-most part of Oneida Lake is included in the area, but not the Finger Lakes, with their much deeper waters. For the Crescent Lake area, while the PPS values

came from North Platte, all other meteorological variables were from Scottsbluff (where the PPS values were missing) which is just west of the Wildlife Refuge and is closer than North Platte.

4. Results and Discussions

[23] Figure 3 displays the quasi-time series of monthly evaporation rates estimated by the WSE- and CR-based methods for the warm seasons (June–November or June–October) of the period starting in 2000 and ending in 2006 (2005 at Little Rock). The range and seasonal change of the two estimates are very similar. Indeed, the warm-season-averaged mean monthly evaporation rates differ by less than 5% for each station (Table 2), except at North Platte, where the difference is 7%. The two monthly estimates show a very high correlation with $R^2 = 0.95$ and scatter along the unit slope line (Figure 4). The WSE-based estimates are slightly lower at large values and somewhat higher at small ones in comparison with the traditional CR-based method resulting in a best-fit line slope of 0.83 and intercept 18.45 mm/month. Even the warm-season summed values, to exclude seasonality effects, have the same R^2 value of 0.95 (Figure 5), again scattered along the 1:1 line with a best-fit line slope of 0.89 and intercept of 67.62 mm/warm season.

[24] From these results it can be concluded, that the two evaporation estimation methods, one based on the WSE, the other on the complementary relationship based AA model, yield very similar evaporation estimates, at least at a monthly timescale here employed. This however, is not totally unexpected, since the two methods stem from the same basic assumption: the assumed constancy of the available energy, Q_n , during the drying of the environment. While the current WSE-based method automatically results from the analytical solution of the coupled 2-D turbulent heat and vapor transport equations under certain restrictive conditions, traditional CR-based approaches need some additional considerations. The latter may further assume a symmetric relationship in the temporal change of actual and potential evaporation (PE) rates, which can be expected, provided PE is defined by the Penman equation with its original, Rome wind function [Brutsaert and Stricker, 1979; Szilagyi and Jozsa, 2008]. If an additional reference evaporation rate is defined too, i.e., the wet environment evaporation (PE_0), by the Priestley-Taylor equation [Priestley and Taylor, 1972], then the CR becomes $E + PE = 2PE_0$. This approach of regional evaporation estimation has become known as the Advection-Aridity (AA) model by Brutsaert and Stricker [1979]. A few years later Morton [1983] has defined the terms in the CR differently from the AA model, and his model became known as WREVAP or CRAE [Morton et al., 1985]. For the PE term he employs class-A pan measurements, or in the lack of them, an estimation algorithm he worked out. Class-A pan data (or their estimates) however would alter the symmetry of the CR for reasons (probably unrecognized by Morton) explained by Kahler and Brutsaert [2006] and Szilagyi [2007], so Morton modified the Priestley-Taylor equation empirically to keep the symmetry of the CR, as defined by AA. On a long-term annual basis at least, the two approaches (i.e., AA and WREVAP) of the CR give almost identical results [Szilagyi and Jozsa, 2008], so one is

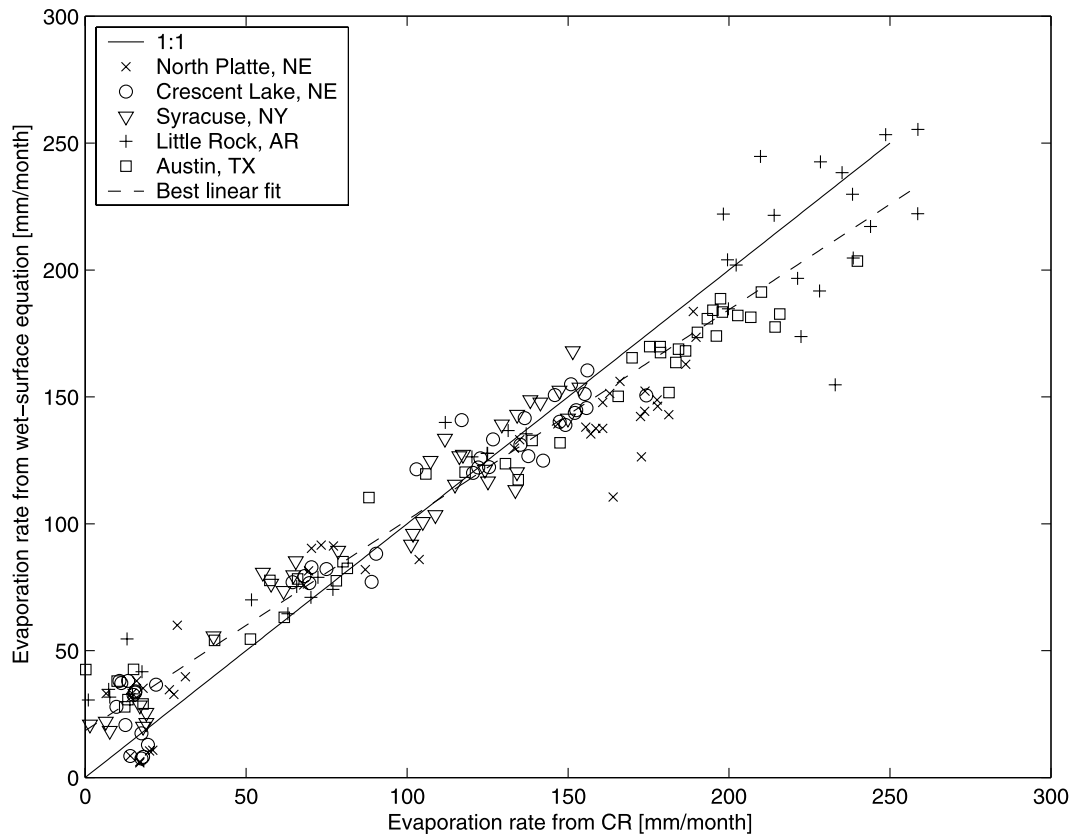


Figure 4. Scatterplot of the CR-based AA model and WSE-based monthly (warm period) evaporation values. $R^2 = 0.95$; the best linear fit has a slope of 0.83 and an intercept value of 18.45 mm/month.

justified to choose either of them. Here the AA model was selected because it requires an additional piece of information about the state of the environment, i.e., wind measurements (which were available), while the WREVP model does not, therefore the former can be expected to yield a stronger correlation with the current method.

[25] There is a clear duality between the two methods (i.e., WSE-based and traditional CR-based): both require net radiation, air temperature, and humidity data. The current method additionally requires drying and wet LST values, the traditional CR-based needs some measure of PE and the wet environment evaporation rate. So while the WSE-based method infers actual evaporation from the difference between drying and wet-surface temperatures, the CR-based performs the same task relying on the difference between potential and wet environment evaporation rates.

[26] The included sensitivity analysis (Figure 6), performed with characteristic mean values for North Platte, Nebraska indicates that the WSE-based evaporation estimation approach is most sensitive to an underestimation of the wet-surface temperature (T_s) value and similarly, but to a lesser degree, to an overestimation of the daytime air temperature (T_{dt}) value. Also, the evaporation estimates are linearly related to Q_n and T_{as} , and are least sensitive to the accuracy of the daytime relative humidity values, RH_{dt} .

5. Summary and Conclusions

[27] The current method of regional evaporation, relying on the coupled 2-D turbulent heat and vapor transport

equations, yields very similar monthly evaporation rates to another regional evaporation estimation method (the AA model by *Brutsaert and Stricker* [1979]) based on the complementary relationship [*Bouchet*, 1963] of evaporation. While both approaches can be used to validate other, possibly more empirical evaporation estimation techniques at a regional scale, the current approach explicitly relates the change in surface temperature to a change in the moisture content of the surface by equation (11), named here the wet-surface equation. In remote-sensing-based evaporation estimation methods, the specification of the vapor pressure at the drying surface is typically one of the most challenging tasks. While WSE has been known for several decades, at least since the publication of *Yeh and Brutsaert* [1971], to the best knowledge of the authors, no one has yet taken advantage of it among the recently dynamically developing evaporation estimation approaches that typically rely on satellite-derived land surface temperature data. The major attractiveness of equation (11) is that it does not contain any tunable parameters, so it may help with the calibration of other techniques that do.

[28] It should be emphasized that the validity of equation (11) holds (as a result of the assumptions employed in its derivation) for a region—which is devoid of sudden large-scale jumps in land-cover characteristics, such as a shoreline—as a whole, and not over the field scale. So without additional further testing and probable necessary modifications, equation (11) should not directly be used to derive the specific humidity (or vapor pressure) over different agricultural plots and thus the evaporation

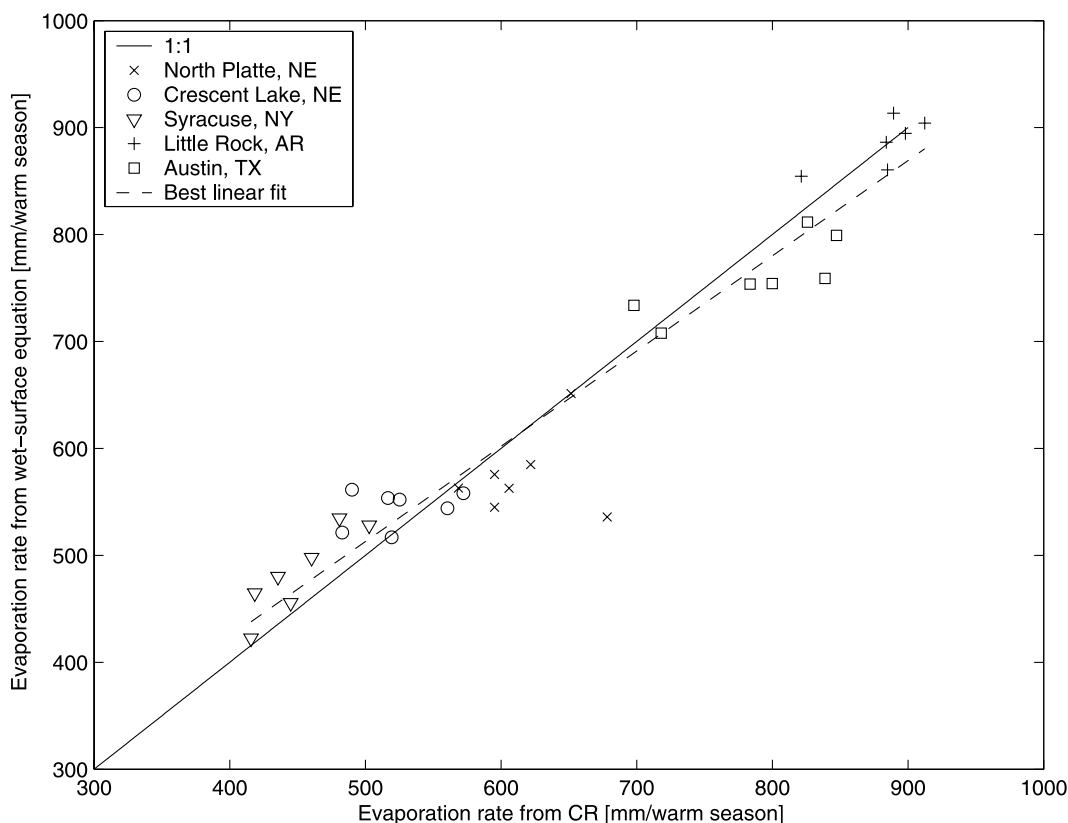


Figure 5. Scatterplot of the CR-based AA and WSE-based warm-period summed evaporation values. $R^2 = 0.95$; the best linear fit has a slope of 0.89 and an intercept value of 67.62 mm/warm season. The correlation coefficients (%) for the individual stations (listed after legend) are 19, 31, 90, 73, 81, all positive.

rates from those fields. While such an extension may be quite possible, as the success of other, perhaps more empirical methods indicate, it needs appropriate further testing, which was not the planned focus of the present study.

[29] The other attractiveness of the present approach (due to the right side of WSE) is that the wet surface does not need to be situated in the footprint area of the atmospheric measurements, since the reference wet-surface temperature (under the prevailing horizontal wind velocity and turbulent diffusivity profiles) is predominantly affected by the available energy only, and not by the aridity of the environment around it. This statement, however, may be true only as long as the area of the wet surface is not too small (i.e., not much smaller than a few hundred meters), since with a reduction in size, local heat transport can play an increasingly important role [Kahler and Brutsaert, 2006; Szilagyi and Jozsa, 2008], demonstrated by the difference in class-A pan and the original Penman-equation-derived evaporation rates. This heat transfer, exemplified as the heating of the side of the class-A pan by the warmer air colliding with it (or a similar heat conduction in the soil across the warmer, drier, and cooler, wetter soil interface), has been excluded from the present formulation of the coupled heat and vapor transport equations.

[30] Accumulating empirical evidence of an existence of the CR [Brutsaert and Parlange, 1998; Ramirez et al.,

2005] as well as the continued success of the CR-based evaporation estimates [Nishida et al., 2003; Ozdogan and Salvucci, 2004; Crago and Crowley, 2005; Brutsaert, 2006; Kahler and Brutsaert, 2006; Szilagyi, 2001, 2007; Szilagyi and Jozsa, 2008] suggest that the assumptions (especially a spatially and temporally near-constant net energy term) in the derivation (common with the CR-based methods) of the present WSE-based evaporation method may not be unrealistic in practice. This is due, presumably, to a not too dramatic difference in albedo of the vegetated and open-water surfaces for the regions studied, which, however, could be more significant in sparsely vegetated semiarid regions.

[31] One should also note that by the increase of the averaging period it becomes more likely that the mean behavior of $q(T_{as})$ at the drying land surface will follow the trajectory described in equation (11), since passing weather fronts may alter (e.g., by transporting extra moisture over the area, thus fully or partially decoupling the temperature/moisture status of the land and the adjacent air) the equilibrium state of the drying land-atmosphere system only temporarily. Also, over a longer period, the alternating processes of rewetting and drying of the environment may occur in a larger number ultimately resulting in a mean behavior of the system according to equation (11), even if none of the individual drying events may exactly follow equation (11). For this reason (i.e., to avoid the effects of passing fronts), it may be advisable not to apply the present

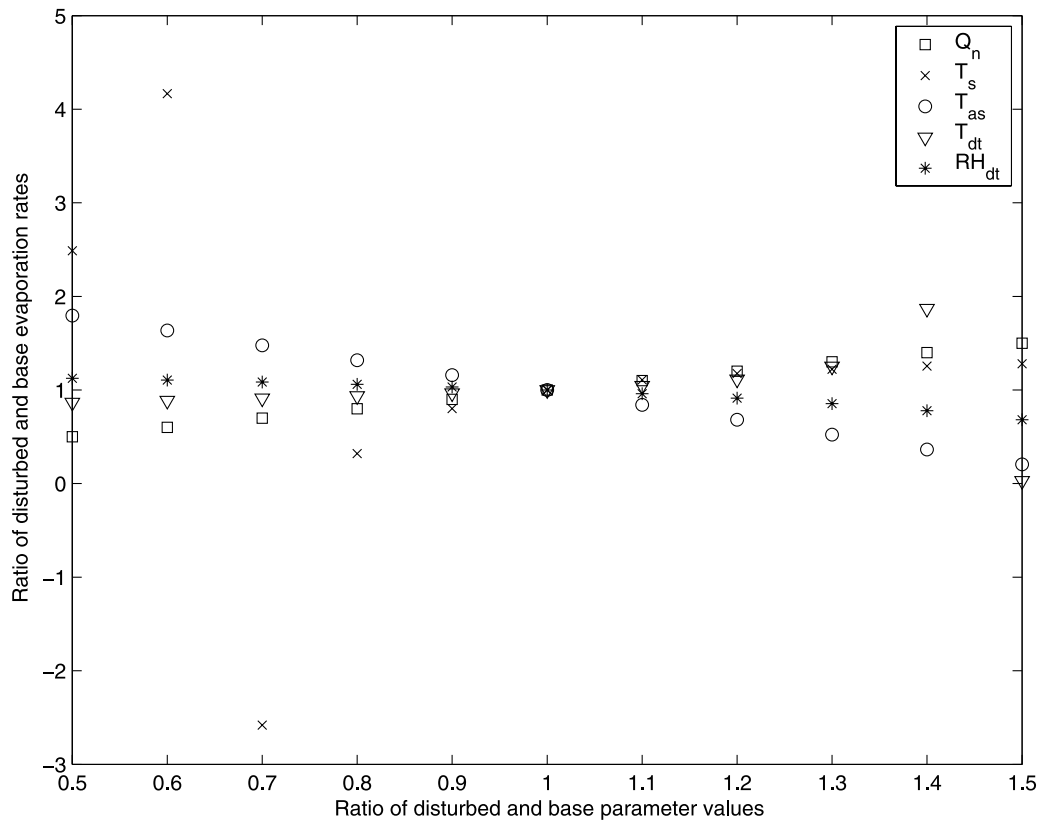


Figure 6. Sensitivity analysis of the WSE-based evaporation estimates. The base values of the variables are characteristic mean monthly values for North Platte, Nebraska. $Q_n = 130$ mm/month, $T_s = 23^\circ\text{C}$, $T_{as} = 27^\circ\text{C}$, $T_{dt} = 20^\circ\text{C}$, $RH_{dt} = 0.6$, resulting in an evaporation rate of 92 mm/month.

method (as any CR-based method) over periods shorter than 5–7 days, as has been recommended by Morton *et al.* [1985], or when it is done so, to avoid such weather patterns.

[32] **Acknowledgments.** This work has partially been supported by the European Union's Climate Change and Variability: Impact on Central and Eastern Europe (CLAVIER) FP6 project. The authors are grateful to the three anonymous reviewers whose comments greatly improved the manuscript.

References

- Agam, N., W. P. Kustas, M. C. Anderson, F. Li, and P. D. Colaizzi (2008), Utility of thermal image sharpening for monitoring field-scale evapotranspiration over rainfed and irrigated agricultural regions, *Geophys. Res. Lett.*, *35*, L02402, doi:10.1029/2007GL032195.
- Albertson, J. D., and M. B. Parlange (1999), Natural integration of scalar fluxes from complex terrain, *Adv. Water Resour.*, *23*(3), 239–252.
- Albertson, J. D., W. P. Kustas, and T. M. Scanlon (2001), Large-eddy simulation over heterogeneous terrain with remotely sensed land surface conditions, *Water Resour. Res.*, *37*, 1939–1953.
- Allen, R. G., T. Masahiro, A. Morse, R. Trezza, J. L. Wright, W. Bastiaanssen, W. Kramber, I. Lorite, and C. W. Robison (2007), Satellite-based energy balance for mapping evapotranspiration with internalized calibration (METRIC)—Applications, *J. Irrig. Drain. Eng.*, *133*(4), 395–406.
- Anderson, M. C., W. P. Kustas, and J. M. Norman (2007), Upscaling flux observations from local to continental scales using thermal remote sensing, *Agron. J.*, *99*, 240–254.
- Bouchet, R. J. (1963), Evapotranspiration réelle, evapotranspiration potentielle, et production agricole, *Ann. Agron.*, *14*, 543–824.
- Brutsaert, W. (1982), *Evaporation Into the Atmosphere*, Springer, New York.
- Brutsaert, W. (2006), Indications of increasing land-surface evaporation during the second half of the 20th century, *Geophys. Res. Lett.*, *33*, L20403, doi:10.1029/2006GL027532.
- Brutsaert, W., and H. Stricker (1979), An advection-aridity approach to estimate actual regional evapotranspiration, *Water Resour. Res.*, *15*, 443–449.
- Brutsaert, W., and M. B. Parlange (1998), Hydrologic cycle explains the evaporation paradox, *Nature*, *396*, 30.
- Courault, D., B. Seguin, and A. Olioso (2005), Review on estimation of evapotranspiration from remote sensing data: From empirical to numerical modeling approaches, *Irrig. Drain. Syst.*, *19*(3–4), 223–249.
- Crago, R., and R. Crowley (2005), Complementary relationships for near-instantaneous evaporation, *J. Hydrol.*, *300*, 199–211.
- Gowda, P. H., J. L. Chavez, P. D. Colaizzi, S. R. Evett, T. A. Howell, and J. A. Tolc (2008), ET mapping for agricultural water management: Present status and challenges, *Irrig. Sci.*, *26*(3), 223–237.
- Kahler, D. M., and W. Brutsaert (2006), Complementary relationship between daily evaporation in the environment and pan evaporation, *Water Resour. Res.*, *42*, W05413, doi:10.1029/2005WR004541.
- Kustas, W. P., and J. D. Albertson (2003), Effects of surface temperature contrast on land-atmosphere exchange: A case study from Monsoon 90, *Water Resour. Res.*, *39*(6), 1159, doi:10.1029/2001WR001226.
- Laikhtman, D. L. (1964), *Physics of the Boundary Layer of the Atmosphere*, Sivan Press, Israel.
- Leclerc, M. Y., S. H. Shen, and B. Lamb (1997), Observations and large-eddy simulation modeling of footprints in the lower convective boundary layer, *J. Geophys. Res.*, *102*, 9323–9334.
- Maidment, D. R. (Ed.) (1993), *Handbook of Hydrology*, McGraw-Hill, New York.
- Morton, F. I. (1983), Operational estimates of areal evapotranspiration and their significance to the science and practice of hydrology, *J. Hydrol.*, *66*, 1–76.
- Morton, F. I., F. Ricard, and S. Fogarasi (1985), Operational estimates of areal evapotranspiration and lake evaporation—Program WREVAP, *NHRI Pap. 24*, National Hydrological Research Institute, Ottawa, ON, Canada.
- Nishida, K., R. R. Nemani, S. W. Running, and J. M. Glassy (2003), An operational remote sensing algorithm of land surface evaporation, *J. Geophys. Res.*, *108*(D9), 4270, doi:10.1029/2002JD002062.

- Ozdogan, M., and G. D. Salvucci (2004), Irrigation-induced changes in potential evapotranspiration in south-eastern Turkey: Test and application of Bouchet's complementary hypothesis, *Water Resour. Res.*, *40*, W04301, doi:10.1029/2003WR002822.
- Priestley, C. H. B., and R. J. Taylor (1972), On the assessment of surface heat flux and evaporation using large-scale parameters, *Mon. Weather Rev.*, *100*, 81–92.
- Ramirez, J. A., M. T. Hobbins, and T. C. Brown (2005), Observational evidence of the complementary relationship in regional evaporation lends strong support for Bouchet's hypothesis, *Geophys. Res. Lett.*, *32*, L15401, doi:10.1029/2005GL023549.
- Szilagyi, J. (2001), Modeled areal evaporation trends over the conterminous United States, *J. Irrig. Drain. Eng.*, *127*(4), 196–200.
- Szilagyi, J. (2007), On the inherent asymmetric nature of the complementary relationship of evaporation, *Geophys. Res. Lett.*, *34*, L02405, doi:10.1029/2006GL028708.
- Szilagyi, J., and J. Jozsa (2008), New findings about the complementary relationship-based evaporation estimation methods, *J. Hydrol.*, *354*, 171–186.
- Yeh, G.-T., and W. Brutsaert (1971), A solution for simultaneous turbulent heat and vapor transfer between a water surface and the atmosphere, *Bound. Layer Meteorol.*, *2*, 64–82.

J. Jozsa, Department of Hydraulic and Water Resources Engineering, Budapest University of Technology and Economics, H-1111 Muegyetem Rkp. 3-9, Budapest, Hungary.

J. Szilagyi, School of Natural Resources, Lincoln Conservation and Survey Division, University of Nebraska, 113 Nebraska Hall, 901 N. 17th Street, P.O. Box 880517, Lincoln, NE 68588-0517, USA. (jszilagyi1@unl.edu)